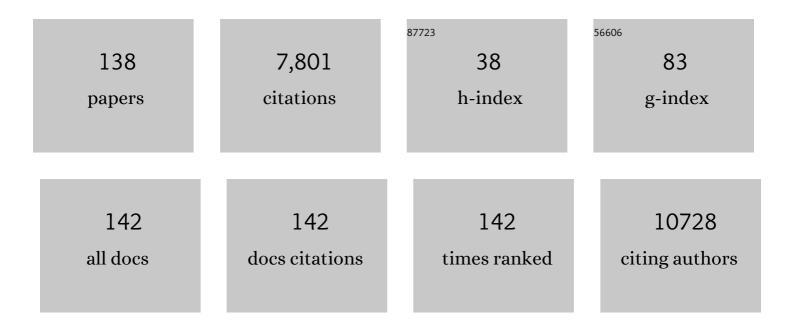
## Hae-Jeong Park

List of Publications by Year in descending order

Source: https://exaly.com/author-pdf/4613681/publications.pdf Version: 2024-02-01



HAE-LEONC DADK

#	Article	IF	CITATIONS
1	A populational connection distribution map for the whole brain white matter reveals ordered cortical wiring in the space of white matter. NeuroImage, 2022, 254, 119167.	2.1	2
2	Analyzing differences between parent- and self-report measures with a latent space approach. PLoS ONE, 2022, 17, e0269376.	1.1	0
3	Re-visiting Riemannian geometry of symmetric positive definite matrices for the analysis of functional connectivity. NeuroImage, 2021, 225, 117464.	2.1	35
4	A computational framework for optimal control of a self-adjustive neural system with activity-dependent and homeostatic plasticity. NeuroImage, 2021, 230, 117805.	2.1	2
5	A Computational Framework for Controlling the Self-Restorative Brain Based on the Free Energy and Degeneracy Principles. Frontiers in Computational Neuroscience, 2021, 15, 590019.	1.2	3
6	Bayesian estimation of maximum entropy model for individualized energy landscape analysis of brain state dynamics. Human Brain Mapping, 2021, 42, 3411-3428.	1.9	7
7	Bayesian adaptive model estimation to solve the speed accuracy tradeoff problem in psychophysical experiments. Scientific Reports, 2021, 11, 18264.	1.6	2
8	Empirical Bayes estimation of pairwise maximum entropy model for nonlinear brain state dynamics. Neurolmage, 2021, 244, 118618.	2.1	4
9	Differential Biases and Variabilities of Deep Learning–Based Artificial Intelligence and Human Experts in Clinical Diagnosis: Retrospective Cohort and Survey Study. JMIR Medical Informatics, 2021, 9, e33049.	1.3	5
10	State-Dependent Effective Connectivity in Resting-State fMRI. Frontiers in Neural Circuits, 2021, 15, 719364.	1.4	4
11	Inter-species cortical registration between macaques and humans using a functional network property under a spherical demons framework. PLoS ONE, 2021, 16, e0258992.	1.1	0
12	Differential structure-function network coupling in the inattentive and combined types of attention deficit hyperactivity disorder. PLoS ONE, 2021, 16, e0260295.	1.1	6
13	Validation of a mobile game-based assessment of cognitive control among children and adolescents. PLoS ONE, 2020, 15, e0230498.	1.1	15
14	Dynamic causal modeling of hippocampal activity measured via mesoscopic voltage-sensitive dye imaging. Neurolmage, 2020, 213, 116755.	2.1	1
15	Changes of Neurotransmitters in Youth with Internet and Smartphone Addiction: A Comparison with Healthy Controls and Changes after Cognitive Behavioral Therapy. American Journal of Neuroradiology, 2020, 41, 1293-1301.	1.2	17
16	Neural correlates of anxiety under interrogation in guilt or innocence contexts. PLoS ONE, 2020, 15, e0230837.	1.1	0
17	Dynamic causal modeling for calcium imaging: Exploration of differential effective connectivity for sensory processing in a barrel cortical column. NeuroImage, 2019, 201, 116008.	2.1	4
18	Automated diagnosis of ear disease using ensemble deep learning with a big otoendoscopy image database. EBioMedicine, 2019, 45, 606-614.	2.7	97

#	Article	IF	CITATIONS
19	Graph-theoretical analysis for energy landscape reveals the organization of state transitions in the resting-state human cerebral cortex. PLoS ONE, 2019, 14, e0222161.	1.1	21
20	Neurofeedback learning for mental practice rather than repetitive practice improves neural pattern consistency and functional network efficiency in the subsequent mental motor execution. NeuroImage, 2019, 188, 680-693.	2.1	6
21	Effective connectivity during working memory and resting states: A DCM study. NeuroImage, 2018, 169, 485-495.	2.1	31
22	Dynamic effective connectivity in resting state fMRI. NeuroImage, 2018, 180, 594-608.	2.1	100
23	Interregional metabolic connectivity of 2â€deoxyâ€2[ <sup>18</sup> F]fluoroâ€Dâ€glucose positron emission tomography in vagus nerve stimulation for pediatric patients with epilepsy: A retrospective crossâ€sectional study. Epilepsia, 2018, 59, 2249-2259.	2.6	13
24	Aberrant cerebro-cerebellar functional connectivity and minimal self-disturbance in individuals at ultra-high risk for psychosis and with first-episode schizophrenia. Schizophrenia Research, 2018, 202, 138-140.	1.1	19
25	Involvement of amygdala–prefrontal dysfunction in the influence of negative emotion on the resolution of cognitive conflict in patients with schizophrenia. Brain and Behavior, 2018, 8, e01064.	1.0	9
26	Geometric Convolutional Neural Network for Analyzing Surface-Based Neuroimaging Data. Frontiers in Neuroinformatics, 2018, 12, 42.	1.3	29
27	Individuality manifests in the dynamic reconfiguration of large-scale brain networks during movie viewing. Scientific Reports, 2017, 7, 41414.	1.6	21
28	Energy landscape analysis of the subcortical brain network unravels system properties beneath resting state dynamics. Neurolmage, 2017, 149, 153-164.	2.1	29
29	Aberrant neural networks for the recognition memory of socially relevant information in patients with schizophrenia. Brain and Behavior, 2017, 7, e00602.	1.0	9
30	Large-scale DCMs for resting-state fMRI. Network Neuroscience, 2017, 1, 222-241.	1.4	146
31	Contribution of fronto-striatal regions to emotional valence and repetition under cognitive conflict. Brain Research, 2017, 1666, 48-57.	1.1	10
32	Changes in brain metabolic connectivity underlie autistic-like social deficits in a rat model of autism spectrum disorder. Scientific Reports, 2017, 7, 13213.	1.6	30
33	Analysis of structure–function network decoupling in the brain systems of spastic diplegic cerebral palsy. Human Brain Mapping, 2017, 38, 5292-5306.	1.9	28
34	Comparative evaluation of the white matter fiber integrity in patients with prelingual and postlingual deafness. NeuroReport, 2017, 28, 1103-1107.	0.6	8
35	Hierarchical Dynamic Causal Modeling of Resting-State fMRI Reveals Longitudinal Changes in Effective Connectivity in the Motor System after Thalamotomy for Essential Tremor. Frontiers in Neurology, 2017, 8, 346.	1.1	36
36	Structural Brain Connectivity Constrains within-a-Day Variability of Direct Functional Connectivity. Frontiers in Human Neuroscience, 2017, 11, 408.	1.0	11

#	Article	IF	CITATIONS
37	Multivariate Bayesian decoding of single-trial event-related fMRI responses for memory retrieval of voluntary actions. PLoS ONE, 2017, 12, e0182657.	1.1	1
38	Immediate and Longitudinal Alterations of Functional Networks after Thalamotomy in Essential Tremor. Frontiers in Neurology, 2016, 7, 184.	1.1	34
39	PM456. Aberrant cortico-cerebellar connectivity of the default mode network in individuals at ultra-high risk for psychosis: a resting-state fMRI study. International Journal of Neuropsychopharmacology, 2016, 19, 65-66.	1.0	0
40	Neural responses to affective and cognitive theory of mind in children and adolescents with autism spectrum disorder. Neuroscience Letters, 2016, 621, 117-125.	1.0	26
41	Connectivity-based change point detection for large-size functional networks. NeuroImage, 2016, 143, 353-363.	2.1	27
42	Happier People Show Greater Neural Connectivity during Negative Self-Referential Processing. PLoS ONE, 2016, 11, e0149554.	1.1	11
43	A Study on the Neurobiological Basis of Communicative Intelligence Using Voxel-Based Morphometry. Korean Journal of Schizophrenia Research, 2015, 18, 35.	0.3	0
44	A Network Analysis of <sup>15</sup> O-H <sub>2</sub> O PET Reveals Deep Brain Stimulation Effects on Brain Network of Parkinson's Disease. Yonsei Medical Journal, 2015, 56, 726.	0.9	10
45	The neural basis of a deficit in abstract thinking in patients with schizophrenia. Psychiatry Research - Neuroimaging, 2015, 234, 66-73.	0.9	13
46	Altered cingulo-striatal function underlies reward drive deficits in schizophrenia. Schizophrenia Research, 2015, 161, 229-236.	1.1	28
47	Multivariate detrending of fMRI signal drifts for real-time multiclass pattern classification. NeuroImage, 2015, 108, 203-213.	2.1	6
48	Motion correction of magnetic resonance imaging data by using adaptive moving least squares method. Magnetic Resonance Imaging, 2015, 33, 659-670.	1.0	2
49	Graph Independent Component Analysis Reveals Repertoires of Intrinsic Network Components in the Human Brain. PLoS ONE, 2014, 9, e82873.	1.1	20
50	Abnormal Neural Processing during Emotional Salience Attribution of Affective Asymmetry in Patients with Schizophrenia. PLoS ONE, 2014, 9, e90792.	1.1	21
51	Involvement of the mirror neuron system in blunted affect in schizophrenia. Schizophrenia Research, 2014, 152, 268-274.	1.1	40
52	Reduced Binding Potential of GABA-A/Benzodiazepine Receptors in Individuals at Ultra-high Risk for Psychosis: An [18F]-Fluoroflumazenil Positron Emission Tomography Study. Schizophrenia Bulletin, 2014, 40, 548-557.	2.3	33
53	Positive symptoms and water diffusivity of the prefrontal and temporal cortices in schizophrenia patients: A pilot study. Psychiatry Research - Neuroimaging, 2014, 224, 49-57.	0.9	14
54	Functional network organizations of two contrasting temperament groups in dimensions of novelty seeking and harm avoidance. Brain Research, 2014, 1575, 33-44.	1.1	24

#	Article	IF	CITATIONS
55	Histogram Analysis of Gadoxetic Acid-Enhanced MRI for Quantitative Hepatic Fibrosis Measurement. PLoS ONE, 2014, 9, e114224.	1.1	25
56	Functional connectivityâ€based identification of subdivisions of the basal ganglia and thalamus using multilevel independent component analysis of resting state fMRI. Human Brain Mapping, 2013, 34, 1371-1385.	1.9	77
57	Perceived patient–parent relationships and neural representation of parents in schizophrenia. European Archives of Psychiatry and Clinical Neuroscience, 2013, 263, 259-269.	1.8	3
58	Structural and Functional Brain Networks: From Connections to Cognition. Science, 2013, 342, 1238411.	6.0	1,543
59	Everyday conversation requires cognitive inference: Neural bases of comprehending implicated meanings in conversations. NeuroImage, 2013, 81, 61-72.	2.1	45
60	Increased GABA-A Receptor Binding and Reduced Connectivity at the Motor Cortex in Children with Hemiplegic Cerebral Palsy: A Multimodal Investigation Using <sup>18</sup> F-Fluoroflumazenil PET, Immunohistochemistry, and MR Imaging. Journal of Nuclear Medicine, 2013, 54, 1263-1269.	2.8	23
61	Evaluation of Node-Inhomogeneity Effects on the Functional Brain Network Properties Using an Anatomy-Constrained Hierarchical Brain Parcellation. PLoS ONE, 2013, 8, e74935.	1.1	19
62	Correlations of Dynamic Contrast-Enhanced Magnetic Resonance Imaging with Morphologic, Angiogenic, and Molecular Prognostic Factors in Rectal Cancer. Yonsei Medical Journal, 2013, 54, 123.	0.9	27
63	Is the GABA System Related to the Social Competence Improvement Effect of Aripiprazole? An <sup>18</sup> F-Fluoroflumazenil PET Study. Psychiatry Investigation, 2013, 10, 75.	0.7	19
64	Regional cerebral blood flow changes and performance deficit during a sustained attention task in schizophrenia: <sup>15</sup> <scp>O</scp> â€ <scp>w</scp> ater positron emission tomography. Psychiatry and Clinical Neurosciences, 2012, 66, 564-572.	1.0	4
65	Hippocampus and nucleus accumbens activity during neutral word recognition related to trait physical anhedonia in patients with schizophrenia: An fMRI study. Psychiatry Research - Neuroimaging, 2012, 203, 46-53.	0.9	21
66	Common and differential brain responses in men and women to nonverbal emotional vocalizations by the same and opposite sex. Neuroscience Letters, 2012, 515, 157-161.	1.0	14
67	Alpha amplitude and phase locking in obsessive-compulsive disorder during working memory. International Journal of Psychophysiology, 2012, 83, 1-7.	0.5	11
68	Are brain networks stable during a 24-hour period?. NeuroImage, 2012, 59, 456-466.	2.1	47
69	A randomized trial of mesenchymal stem cells in multiple system atrophy. Annals of Neurology, 2012, 72, 32-40.	2.8	199
70	Distortion correction of high b-valued and high angular resolution diffusion images using iterative simulated images. Neurolmage, 2011, 57, 968-978.	2.1	21
71	Consonant chords stimulate higher EEG gamma activity than dissonant chords. Neuroscience Letters, 2011, 488, 101-105.	1.0	11
72	Neuroanatomical correlates of trait anhedonia in patients with schizophrenia: A voxel-based morphometric study. Neuroscience Letters, 2011, 489, 110-114.	1.0	28

#	Article	IF	CITATIONS
73	Prestimulus top-down reflection of obsessive-compulsive disorder in EEG frontal theta and occipital alpha oscillations. Neuroscience Letters, 2011, 496, 181-185.	1.0	26
74	Activation of the Occipital Cortex and Deactivation of the Default Mode Network During Working Memory in the Early Blind. Journal of the International Neuropsychological Society, 2011, 17, 407-422.	1.2	24
75	Neural correlates in the processing of phoneme-level complexity in vowel production. Brain and Language, 2011, 119, 158-166.	0.8	15
76	Decoding brain states using functional magnetic resonance imaging. Biomedical Engineering Letters, 2011, 1, 82-88.	2.1	7
77	The pattern of cortical atrophy in patients with Parkinson's disease according to cognitive status. Movement Disorders, 2011, 26, 289-296.	2.2	131
78	A method for anisotropic spatial smoothing of functional magnetic resonance images using distance transformation of a structural image. Physics in Medicine and Biology, 2011, 56, 5063-5077.	1.6	6
79	Motor pathway injury in patients with periventricular leucomalacia and spastic diplegia. Brain, 2011, 134, 1199-1210.	3.7	113
80	The frontal and temporal lobe in the identification of laryngeal contrasts. NeuroReport, 2010, 21, 474-478.	0.6	6
81	Task-related modulation of anterior theta and posterior alpha EEG reflects top-down preparation. BMC Neuroscience, 2010, 11, 79.	0.8	67
82	A comparison of gray and white matter density in patients with Parkinson's disease dementia and dementia with Lewy bodies using voxelâ€based morphometry. Movement Disorders, 2010, 25, 28-34.	2.2	57
83	A comparative analysis of cognitive profiles and white-matter alterations using voxel-based diffusion tensor imaging between patients with Parkinson's disease dementia and dementia with Lewy bodies. Journal of Neurology, Neurosurgery and Psychiatry, 2010, 81, 320-326.	0.9	93
84	Real-time functional MRI for patient monitoring during a language task. , 2009, 2009, 5389-92.		1
85	Evaluative processing of ambivalent stimuli in patients with schizophrenia and depression: A [ <sup>15</sup> 0] H <sub>2</sub> 0 PET study. Journal of the International Neuropsychological Society, 2009, 15, 990-1001.	1.2	9
86	Triple-Layer Appearance of Brodmann Area 4 at Thin-Section Double Inversion-Recovery MR Imaging. Radiology, 2009, 250, 515-522.	3.6	20
87	Evaluation of Bayesian tensor estimation using tensor coherence. Physics in Medicine and Biology, 2009, 54, 3785-3802.	1.6	2
88	Medial prefrontal default-mode hypoactivity affecting trait physical anhedonia in schizophrenia. Psychiatry Research - Neuroimaging, 2009, 171, 155-165.	0.9	61
89	Comparison of various imaging modalities in localization of epileptogenic lesion using epilepsy surgery outcome in pediatric patients. Seizure: the Journal of the British Epilepsy Association, 2009, 18, 504-510.	0.9	56
90	Abnormal brain response during the auditory emotional processing in schizophrenic patients with chronic auditory hallucinations. Schizophrenia Research, 2009, 107, 83-91.	1.1	36

#	Article	IF	CITATIONS
91	Morphological alterations in the congenital blind based on the analysis of cortical thickness and surface area. NeuroImage, 2009, 47, 98-106.	2.1	201
92	Alterations of white matter diffusion anisotropy in early deafness. NeuroReport, 2009, 20, 1032-1036.	0.6	57
93	Anhedonia and Ambivalence in Schizophrenic Patients with Fronto-Cerebellar Metabolic Abnormalities: A Fluoro-D-Glucose Positron Emission Tomography Study. Psychiatry Investigation, 2009, 6, 72.	0.7	11
94	Corpus callosal connection mapping using cortical gray matter parcellation and DT-MRI. Human Brain Mapping, 2008, 29, 503-516.	1.9	221
95	Reciprocal activation of the orbitofrontal cortex and the ventrolateral prefrontal cortex in processing ambivalent stimuli. Brain Research, 2008, 1246, 136-143.	1.1	15
96	Prestimulus EEG alpha activity reflects temporal expectancy. Neuroscience Letters, 2008, 438, 270-274.	1.0	25
97	Dysfunctional modulation of emotional interference in the medial prefrontal cortex in patients with schizophrenia. Neuroscience Letters, 2008, 440, 119-124.	1.0	47
98	SENSE factors for reliable cortical thickness measurement. NeuroImage, 2008, 40, 187-196.	2.1	12
99	Prefrontal functional dissociation in the semantic network of patients with schizophrenia. NeuroReport, 2008, 19, 1391-1395.	0.6	4
100	Different hemispheric specializations for pitch and audioverbal working memory. NeuroReport, 2008, 19, 99-103.	0.6	10
101	Quantification of thalamocortical tracts in schizophrenia on probabilistic maps. NeuroReport, 2008, 19, 399-403.	0.6	28
102	Measuring Fractional Anisotropy of the Corpus Callosum Using Diffusion Tensor Imaging: Mid-Sagittal versus Axial Imaging Planes. Korean Journal of Radiology, 2008, 9, 391.	1.5	16
103	Reorganization of neural circuits in the blind on diffusion direction analysis. NeuroReport, 2007, 18, 1757-1760.	0.6	40
104	Visualization of maturation of the corpus callosum during childhood and adolescence using T2 relaxometry. International Journal of Developmental Neuroscience, 2007, 25, 409-414.	0.7	16
105	Assessment of regional GABAA receptor binding using 18F-fluoroflumazenil positron emission tomography in spastic type cerebral palsy. NeuroImage, 2007, 34, 19-25.	2.1	25
106	Volumetric abnormalities in connectivity-based subregions of the thalamus in patients with chronic schizophrenia. Schizophrenia Research, 2007, 97, 226-235.	1.1	33
107	White matter abnormalities associated with auditory hallucinations in schizophrenia: A combined study of voxel-based analyses of diffusion tensor imaging and structural magnetic resonance imaging. Psychiatry Research - Neuroimaging, 2007, 156, 93-104.	0.9	144
108	A review of diffusion tensor imaging studies in schizophrenia. Journal of Psychiatric Research, 2007, 41, 15-30.	1.5	686

#	Article	IF	CITATIONS
109	Increased water diffusivity in the frontal and temporal cortices of schizophrenic patients. NeuroImage, 2006, 30, 1285-1291.	2.1	62
110	Cortical surface-based analysis of 18F-FDG PET: Measured metabolic abnormalities in schizophrenia are affected by cortical structural abnormalities. NeuroImage, 2006, 31, 1434-1444.	2.1	56
111	Fornix Integrity and Hippocampal Volume in Male Schizophrenic Patients. Biological Psychiatry, 2006, 60, 22-31.	0.7	160
112	Relationship between bilateral temporal hypometabolism and EEG findings for mesial temporal lobe epilepsy: Analysis of 18F-FDG PET using SPM. Seizure: the Journal of the British Epilepsy Association, 2006, 15, 56-63.	0.9	46
113	Smaller Neocortical Gray Matter and Larger Sulcal Cerebrospinal Fluid Volumes in Neuroleptic-Naive Women With Schizotypal Personality Disorder. Archives of General Psychiatry, 2006, 63, 1090.	13.8	36
114	How does distortion correction correlate with anisotropic indices? A diffusion tensor imaging study. Magnetic Resonance Imaging, 2006, 24, 1369-1376.	1.0	27
115	Functional disconnection of the semantic networks in schizophrenia. NeuroReport, 2005, 16, 355-359.	0.6	24
116	Sex differences in the human corpus callosum: diffusion tensor imaging study. NeuroReport, 2005, 16, 795-798.	0.6	127
117	Development of Korean Standard Brain Templates. Journal of Korean Medical Science, 2005, 20, 483.	1.1	65
118	Quantification of White Matter using Diffusionâ€Tensor Imaging. International Review of Neurobiology, 2005, 66, 167-212.	0.9	5
119	DTI and MTR abnormalities in schizophrenia: Analysis of white matter integrity. NeuroImage, 2005, 26, 1109-1118.	2.1	399
120	Response to Rosburg: A voxel-based statistical parametric mapping of MMN current densities. Human Brain Mapping, 2004, 21, 46-48.	1.9	3
121	An MRI study of spatial probability brain map differences between first-episode schizophrenia and normal controls. Neurolmage, 2004, 22, 1231-1246.	2.1	40
122	White matter hemisphere asymmetries in healthy subjects and in schizophrenia: a diffusion tensor MRI study. NeuroImage, 2004, 23, 213-223.	2.1	284
123	Clustering Fiber Traces Using Normalized Cuts. Lecture Notes in Computer Science, 2004, , 368-375.	1.0	77
124	Medical Image Computing and Computer-Assisted Intervention – MICCAI 2004. Lecture Notes in Computer Science, 2004, 3216/2004, 368-375.	1.0	54
125	Method for combining information from white matter fiber tracking and gray matter parcellation. American Journal of Neuroradiology, 2004, 25, 1318-24.	1.2	29
126	Optimized individual mismatch negativity source localization using a realistic head model and the Talairach coordinate system. Brain Topography, 2003, 15, 233-238.	0.8	22

#	Article	IF	CITATIONS
127	Independent component model for cognitive functions of multiple subjects using [150]H2O PET images. Human Brain Mapping, 2003, 18, 284-295.	1.9	15
128	Altered hemispheric asymmetry and positive symptoms in schizophrenia: equivalent current dipole of auditory mismatch negativity. Schizophrenia Research, 2003, 59, 253-260.	1.1	97
129	LORETA imaging of P300 in schizophrenia with individual MRI and 128-channel EEG. NeuroImage, 2003, 20, 1552-1560.	2.1	48
130	Spatial normalization of diffusion tensor MRI using multiple channels. NeuroImage, 2003, 20, 1995-2009.	2.1	194
131	Coloring of DT-MRI Fiber Traces Using Laplacian Eigenmaps. Lecture Notes in Computer Science, 2003, , 518-529.	1.0	40
132	Functional Disconnection Between the Prefrontal and Parietal Cortices During Working Memory Processing in Schizophrenia: A [150]H2O PET Study. American Journal of Psychiatry, 2003, 160, 919-923.	4.0	137
133	Automated detection and elimination of periodic ECG artifacts in EEG using the energy interval histogram method. IEEE Transactions on Biomedical Engineering, 2002, 49, 1526-1533.	2.5	63
134	Temporal association of MMN multiple generators: high density recording (128 channels). International Congress Series, 2002, 1232, 335-338.	0.2	1
135	Relationship between personality trait and regional cerebral glucose metabolism assessed with positron emission tomography. Biological Psychology, 2002, 60, 109-120.	1.1	58
136	Statistical parametric mapping of LORETA using high density EEG and individual MRI: Application to mismatch negativities in Schizophrenia. Human Brain Mapping, 2002, 17, 168-178.	1.9	99
137	A study on the elimination of the ECG artifact in the polysomnographic EEG and EOG using AR model. , 0, , .		4
138	A study on the integration and synchronization of video image using H.261 in polysomnography. , 0, , .		0